3618 *J. Med. Chem.* **2010,** *53,* 3618–3625
DOI: 10.1021/jm100039a

Journal of Medicinal Chemistry Article

Discovery, Structure−Activity Relationships, Pharmacokinetics, and Efficacy of Glucokinase Activator (2*R*)-3-Cyclopentyl-2-(4-methanesulfonylphenyl)-*N*-thiazol-2-yl-propionamide (RO0281675)

Nancy-Ellen Haynes,[†] Wendy L. Corbett,[†] Fred T. Bizzarro,[†] Kevin R. Guertin,[†] Darryl W. Hilliard,[†] George W. Holland,[†] Robert F. Kester,[†] Paige E. Mahaney,[†] Lida Qi,[†] Cheryl L. Spence,[§] John Tengi,[†] Mark T. Dvorozniak,[§] Aruna Railkar,[∥] Franz M. Matschinsky,[‡] Joseph F. Grippo,[§] Joseph Grimsby,[§] and Ramakanth Sarabu*,[†]

[†]*Departments of Discovery Chemistry,* [§]*Metabolic and Vascular Diseases,* [∥]*Non-Clinical Drug Safety, and Discovery Technologies, Hoffmann-La Roche Inc., 340 Kingsland Street, Nutley, New Jersey 07110, and* [‡]*Department of Biochemistry and Diabetes Center, University of Pennsylvania School of Medicine, Philadelphia, Pennsylvania 19104*

Received January 12, 2010

Glucokinase (GK) is a glucose sensor that couples glucose metabolism to insulin release. The important role of GK in maintaining glucose homeostasis is illustrated in patients with GK mutations. In this publication, identification of the hit molecule **1** and its SAR development, which led to the discovery of potent allosteric GK activators **9a** and **21a**, is described. Compound **21a** (RO0281675) was used to validate the clinical relevance of targeting GK to treat type 2 diabetes.

Introduction

Maintenance of tight glycemic control requires a complex interplay between an individual's lifestyle, genes, environment, and neuroendocrine and endocrine systems. Defects in the ability of pancreatic β-cells to secrete insulin in response to meals and the diminished capacity of the liver and skeletal muscle to take up glucose in response to insulin represent core pathophysiological defects associated with type 2 diabetes (T2D[a]). Other tissues such as fat cells, gastrointestinal tract, kidney, and brain also contribute to dysglycemia in patients with T2D.[1] As T2D progresses, patients rely on higher doses of antidiabetic agents and multiple oral antidiabetic drugs and progress to exogenous insulin therapy to gain adequate glycemic control. Therefore, more effective therapeutic agents that target multiple pathogenic abnormalities with sustained efficacy represent a major unmet medical need.

Glucokinase (GK), also called hexokinase IV, is a glycolytic enzyme that catalyzes the oxidative phosphorylation of hexoses by ATP. Unlike its isozymes (hexokinases I−III) that are fully saturated at physiologically glucose levels, GK responds functionally to plasma glucose fluctuations observed during preprandial and postprandial periods. This enables pancreatic β-cell GK to function as a molecular sensor that couples changes in blood glucose levels with insulin release to maintain glucose homeostasis. As a sensor, it determines the rate and threshold concentration of glucose (~5 mM in healthy individuals) required to initiate the signaling cascade leading to insulin release. In the liver, GK catalyzes the first step in glucose metabolism and plays an important role in determining net glucose utilization and production in this organ. GK is also expressed in pancreatic α-cells, enteroendocrine K and L cells, glucose excited/glucose inhibited neurons of the hypothalamus and brainstem, and anterior pituitary cells, but its physiological role in these tissues is less well understood.

The enzymatic parameters and activity of GK (k_{cat}, glucose $S_{0.5}$, and positive kinetic cooperativity) are fundamental to its role as a glucose sensor, and this is best illustrated in humans with diseases related to mutations of GK. For instance, loss-of-function mutations in one or both alleles of the GK gene cause maturity onset diabetes of the young type 2 (MODY-2) and permanent neonatal diabetes mellitus, respectively. In contrast, a gain-of-function mutation in a single GK allele causes persistent hyperinsulinemic hypoglycemia of infancy (PHHI) due to excessive insulin release. On the basis of the pivotal role of GK as a glucose sensor in pancreatic β-cells and its key role in regulating glucose production in the liver, allosteric activators of this enzyme are being actively pursued as antidiabetic agents based on the dual effects on augmenting insulin release and suppressing excessive hepatic glucose production.[2−4]

Screening of Roche's compound library led to the identification of **1**, which was shown to increase GK enzymatic activity by 1.5-fold at 24 μM ($SC_{1.5}$). This molecule had desired "lead-like" properties (i.e, low molecular weight and a combination of polar and nonpolar moieties) to warrant further optimization. RO0281675, **21a**, a prototypical GK activator (GKA) that emerged from this effort, causes robust glucose lowering effects in preclinical models of T2D.[5] These findings have stimulated intense interest within the pharmaceutical industry leading to several structural mimics of **21a**.[6,7] Here we report on the optimization of the original screening hit **1**, which led to the identification of two lead molecules, the *N*-acylurea (RO0274375) **9a** and **21a** (Figure 1).

*To whom correspondence should be addressed. Phone: 973-235-3984. Fax: 973-235-2448. E-mail: ramakanth.sarabu@roche.com.

[a] Abbreviations: ATP, adenosine triphosphate; GK, glucokinase; GKA, glucokinase activator; GSIR, glucose-stimulated insulin release; MODY-2, maturity onset diabetes of the young type 2; OGTT, oral glucose tolerance test; PHHI, persistent hyperinsulinemic hypoglycemia of infancy; PK, phramacokinetics; $SC_{1.5}$, concentration of a compound to increase GK activity by 1.5 times; T2D, type 2 diabetes.

 Published on Web 04/21/2010

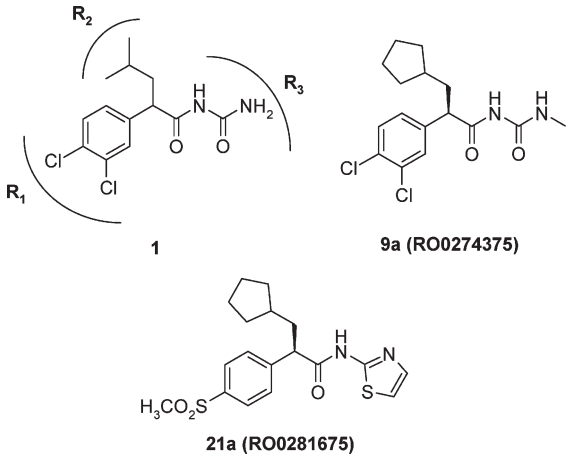

Figure 1. Glucokinase activator hit molecule **1** and optimized molecules **9a** and **21a**.

Chemistry

The target compounds, *N*-acylurea hit **1**, analogues, **5a**−**zf**, and the corresponding 2-aminothiazole amides **8a**−**z** described in this report were prepared following a two to four step sequence outlined in Scheme 1. Starting from commercially available arylacetic acids **2**, direct alkylation or alkylation of the corresponding alkyl ester **6** with an alkyl iodide yielded alkylphenylacetic acids **3** or the esters **7**, respectively. A few ester analogues of **7** were also prepared via the esterification of the corresponding acids **3**. The aryl acetic acid esters **7** were then reacted with urea or alkylureas in the presence of magnesium alkoxide to prepare the unsubstituted, methyl, or ethyl-*N*-acylurea analogues **5**.[8] Additional analogues of **5** containing larger alkyl groups and polar moieties in the R_3 region of the molecule were accessible via the reaction of the phenylacetamide derivative **4** with the appropriate isocyanates.[9] The enantiomers **9a** and **9b** of the racemic **5h** were prepared from stereochemically pure carboxylic acids,

Scheme 1. Synthesis of *N*-Acylurea Analogues[a]

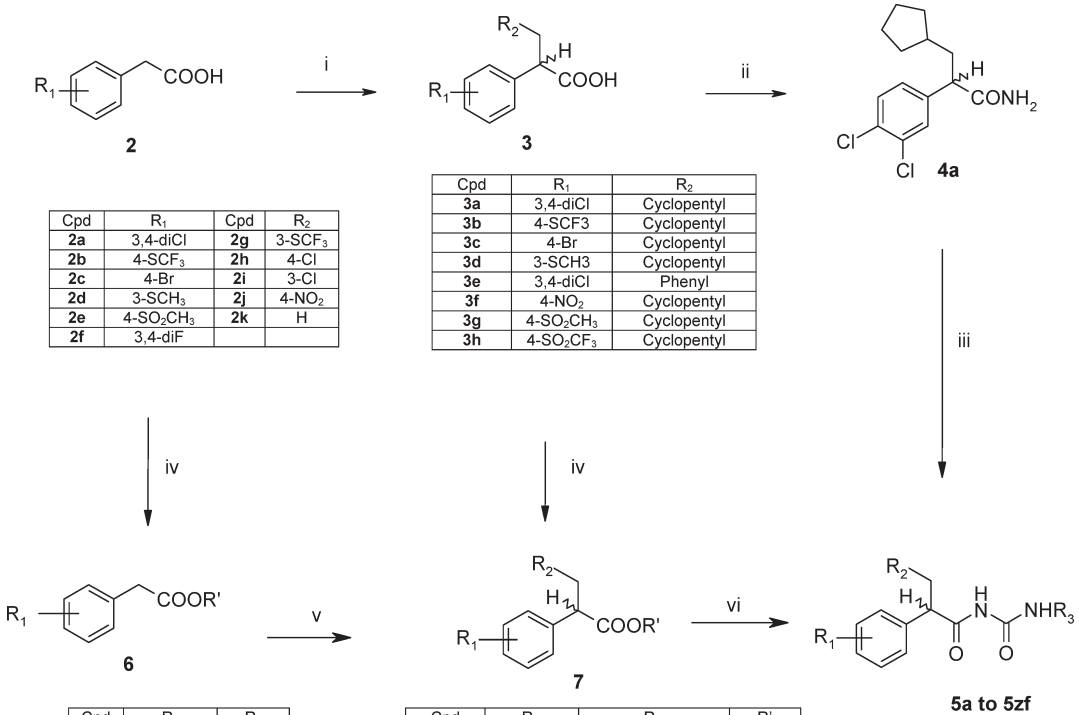

Cpd	R_1	Cpd	R_2
2a	3,4-diCl	**2g**	3-SCF_3
2b	4-SCF_3	**2h**	4-Cl
2c	4-Br	**2i**	3-Cl
2d	3-SCH_3	**2j**	4-NO_2
2e	4-SO_2CH_3	**2k**	H
2f	3,4-diF		

Cpd	R_1	R_2
3a	3,4-diCl	Cyclopentyl
3b	4-SCF3	Cyclopentyl
3c	4-Br	Cyclopentyl
3d	3-SCH3	Cyclopentyl
3e	3,4-diCl	Phenyl
3f	4-NO_2	Cyclopentyl
3g	4-SO_2CH_3	Cyclopentyl
3h	4-SO_2CF_3	Cyclopentyl

Cpd	R_1	R_2
6a	3,4-diCl	CH_3
6b	3-Cl	C_2H_5
6c	4-Cl	C_2H_5
6d	3,4-diF	CH_3
6e	3,4-diCl	C_2H_5
6f	3-SCF_3	CH_3

Cpd	R_1	R_2	R'
7aa	3,4-diCl	Isopropyl	CH_3
7a	3,4-diCl	Isopropyl	C_2H_5
7b	3,4-diCl	Cyclopropyl	CH_3
7c	3,4-diCl	Cyclobutyl	CH_3
7d	3,4-diCl	Cyclopentyl	CH_3
7e	3,4-diCl	Cyclohexyl	CH_3
7f	3,4-diCl	Cycloheptyl	CH_3
7g	3,4-diCl	CH_2-cyclopentyl	C_2H_5
7h	3-Cl	Cyclopentyl	C_2H_5
7i	4-Cl	Cyclopentyl	C_2H_5
7j	H	Cyclopentyl	CH_3
7k	3,4-diF	Cyclopentyl	C_2H_5
7l	4-Br	Cyclopentyl	CH_3
7m	4-NO_2	Cyclopentyl	C_2H_5
7n	4-SCH_3	Cyclopentyl	CH_3
7o	4-SCF_3	Cyclopentyl	CH_3
7p	4-SO_2CH_3	Cyclopentyl	CH_3
7q	4-SO_2CF_3	Cyclopentyl	CH_3
7r	3-SCF_3	Cyclopentyl	CH_3
7s	3-SO_2CF_3	Cyclopentyl	C_2H_5

[a] (i) LDA/HMPA or DMPU, THF, R_2-CH_2-I, −78 °C to room temp; (ii) cat. DMF, $(COCl)_2$, CH_2Cl_2, HMDS, 0 °C to room temp, aq HCl; (iii) $R_3-N=C=O$, toluene, reflux; (iv) cat. H_2SO_4, R′OH, reflux; (v) LDA/HMPA, R_2-CH_2-I; (vi) $Mg(OCH_3)_2$, methyl or ethyl urea, CH_3OH, reflux.

Scheme 2. Synthesis of **9a** and **21a**[a]

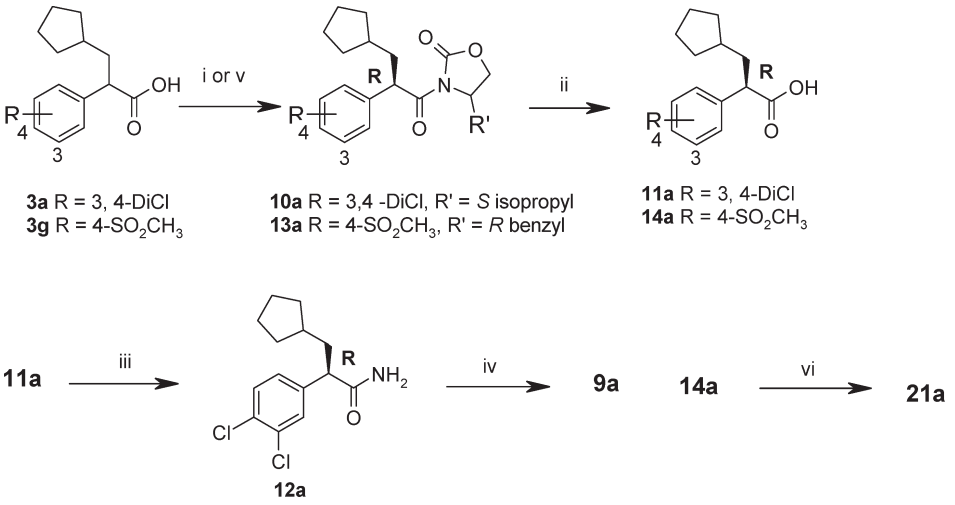

[a] (i) $(CH_3)_3COCl$, Et_3N, then *n*-BuLi, (*S*)-4-isopropyl-2-oxazolidinone, THF 28% (for **3a** to **10a**); (ii) 30% H_2O_2, LiOH, 72% for **11a** and 89% for **14a**; (iii) oxalyl chloride, HMDS, 0 °C, 58%; (iv) MeNCO, toluene, reflux, 63%; (v) $(CH_3)_3COCl$, Et_3N, then *n*-BuLi, (*R*)-4-benzyl-2-oxazolidinone, 49%, (for **3g** to **13a**); (vi) *N*-bromosuccinimide, triphenylphosphine.

Scheme 3. Synthesis of 2-Aminothiazole Amides[a]

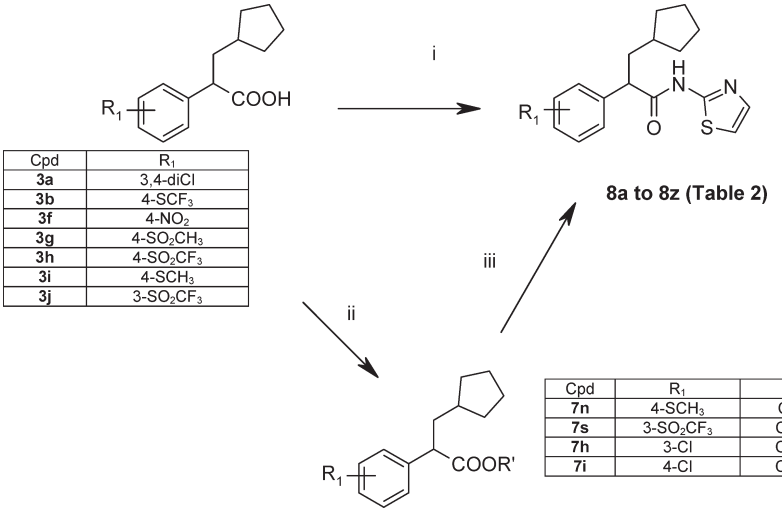

Cpd	R_1
3a	3,4-diCl
3b	4-SCF_3
3f	4-NO_2
3g	4-SO_2CH_3
3h	4-SO_2CF_3
3i	4-SCH_3
3j	3-SO_2CF_3

Cpd	R_1	R'
7n	4-SCH_3	CH_3
7s	3-SO_2CF_3	C_2H_5
7h	3-Cl	C_2H_5
7i	4-Cl	C_2H_5

[a] (i) 2-Aminothiazole, NBS, PPh_3, CH_2Cl_2, room temp; (ii) LiOH, THF/H_2O, room temp; (iii) 2-aminothiazole, $Mg(OCH_3)_2$, CH_3OH, reflux.

11a and **11b**, which were prepared by resolution of the corresponding chiral diastereomeric oxazolidinoneimides **10a** and **10b** (Scheme 2). A single crystal X-ray structure of **9a** was obtained, and the absolute stereochemistry was shown to be *R* (see Figure 1 in Supporting Information). The 2-aminothiazoleamides (**8a**−**z**) were prepared from the arylacetic acids **3** using a *N*-bromosuccinimide/triphenylphosphine coupling method (Scheme 3).[10] Enantiomerically pure **21a** was prepared starting from the corresponding racemic carboxylic acid **3g** via chromatographic separation of diastereomeric benzyloxazolidine derivatives **13a** and **13b**, as shown in Scheme 2. Several structural variants of **5h** were prepared to explore its active conformation.

Results and Discussion

The SAR was explored with the conceptual division of the acylurea hit molecule **1** into three regions around the chiral center: R_1, the substituted aromatic ring; R_2, the alkyl group; R_3, the *N*-acylurea group (Figure 1). Initial studies were centered on the identification of the optimal R_2 alkyl group of the hit molecule **1**. A systematic evaluation of several R_2 analogues that varied in size and polarity were explored (Table 1). The original isopropyl group present in **1** remained the preferred group among the aliphatic groups investigated, while incorporation of cyclohexyl (**5d**) or cyclopentyl (**5c**) moieties were optimal among the alicyclic groups. The latter improved potency by nearly 6-fold over **1**. Larger alkyl, cycloalkyl, aryl groups and groups with polar substitutents significantly reduced activity or were inactive. For example, neopentyl, cyclooctyl, bicyclo[2.2.1]heptyl, 2-methythiazolyl, 4-piperidinyl, and 4-hydroxycyclohexyl analogues were inactive (data not shown). Thus, these studies indicated a clear preference for nonpolar, nonplanar alicyclic groups in the R_2 region of the molecule (Table 1).

The R_1 aromatic group of the hit molecule **1** was explored extensively. The SAR indicated the importance of an aromatic ring with one or two electron withdrawing groups to improve potency and revealed a tolerance for a wide variety of

Table 1. Structure−Activity Relationships of *N*-Acylureas

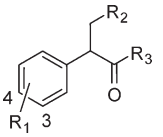

compd	R_1	R_2	R_3	$SC_{1.5}$ (μM)[a]
1	3,4-diCl	isopropyl	$NHCONH_2$	29 ± 7.9 (4)
5a	3,4-diCl	cyclopropyl	$NHCONH_2$	40 ± 6.5 (2)
5b	3,4-diCl	cyclobutyl	$NHCONH_2$	10 ± 0.45 (2)
5c	3,4-diCl	cyclopentyl	$NHCONH_2$	4.4 ± 0.35 (2)
5d	3,4-diCl	cyclohexyl	$NHCONH_2$	8.9 ± 2.6 (3)
5e	3,4-diCl	cycloheptyl	$NHCONH_2$	12 ± 6.5 (2)
5f	3,4-diCl	isopropyl	$NHCONHCH_3$	6
5g	3,4-diCl	cyclohexyl	$NHCONHCH_3$	1.4 ± 0.0 (2)
5h	3,4-diCl	cyclopentyl	$NHCONHCH_3$	1 ± 0.19 (3)
5i	3,4-diCl	cyclopentyl-CH_2	$NHCONHCH_3$	na
5j	3,4-diCl	cyclopentyl	$NHCONHCH_2CH_3$	0.53 ± 0.13 (2)
5k	3,4-diCl	cyclopentyl	$NHCONH(CH_2)_2CH_3$	1.3
5l	3,4-diCl	cyclopentyl	$NHCONHCH_2CH{=}CH_2$	1.3 ± 0.22 (2)
5m	3,4-diCl	cyclopentyl	$NHCONHCH_2CH(CH_3)_2$	6.3
5n	3,4-diCl	cyclopentyl	$NHCONH(CH_2)_3CH_3$	na
5o	3,4-diCl	cyclopentyl	$NHCONHCH_2COOC_2H_5$	1.3 ± 0.25 (2)
5p	3,4-diCl	cyclopentyl	$NHCONHCH_2COOH$	na
5q	3,4-diCl	cyclopentyl	$NHCONHCH_2COOCH_3$	0.55 ± 0.078 (2)
5r	3,4-diCl	cyclopentyl	$NHCONH(CH_2)_2COOC_2H_5$	8.4
5s	3,4-diCl	cyclopentyl	$NHCONH(CH_2)_2COOH$	na
5t	3,4-diCl	cyclopentyl	$NHCONH(CH_2)_2COOCH_3$	3.2
5u	3,4-diCl	cyclopentyl	$NHCONH(CH_2)_2OH$	3.4
5v	3-Cl	cyclopentyl	$NHCONHCH_3$	3.7
5w	4-Cl	cyclopentyl	$NHCONHCH_3$	5.4
5x	H	cyclopentyl	$NHCONHCH_3$	28.2
5y	3,4-diF	cyclopentyl	$NHCONHCH_3$	8.5
5z	4-Br	cyclopentyl	$NHCONHCH_3$	3.8
5za	4-NO_2	cyclopentyl	$NHCONHCH_3$	5.4
5zb	4-SCH_3	cyclopentyl	$NHCONHCH_3$	3.2
5zc	4-SCF_3	cyclopentyl	$NHCONHCH_3$	1.4
5zd	4-SO_2CH_3	cycloopentyl	$NHCONHCH_3$	1.5
5ze	4-SO_2CF_3	cyclopentyl	$NHCONHCH_3$	0.3
5zf	3-SO_2CF_3	cyclopentyl	$NHCONHCH_3$	1
16	3,4-diCl	cyclopentyl	imidazoline-2-one	na
17	3,4-diCl	cyclopentyl	$NHC(=N)NH_2$	na
18	3,4-diCl	cyclopentyl	$N(CH_3)CONH(CH_3)$	na
19	3,4-diCl	isopropyl	$NHCON(CH_3)_2$	na
20	3,4-diCl	cyclopentyl	$NHC(=S)NH(CH_3)$	3.8
9a[b]	3,4-diCl	cyclopentyl	$NHCONHCH_3$	0.41 ± 0.049 (6)
9b[c]	3,4-diCl	cyclopentyl	$NHCONHCH_3$	na

[a] Data reported as mean ± SEM (*n*). The average CV of the assay was 15%, based on an analysis of 452 compounds ($SC_{1.5}$ < 2 μM) assayed in duplicate. na: not active up to 30 μM. [b] *R*-isomer. [c] *S*-isomer.

substituents at the *para*-position. For example, the monochlorophenyl analogues **5v** ($SC_{1.5}$ = 3.7 μM) and **5w** ($SC_{1.5}$ = 5.4 μM) were about 6-fold more potent than the unsubstitued phenyl analogue **5x** ($SC_{1.5}$ = 28 μM), and the 3,4-dichlorophenyl analogue **5h** was about 30-fold more potent. The 4-trifluoromethylsulfonyl derivative **5ze** ($SC_{1.5}$ = 0.3 μM) was among the most active analogues in this series and nearly 100-fold more potent than the unsubstituted **5x**. In general *meta*- or *para*-substitutions were well tolerated, while *ortho*-substitutions, such as *o*-chloro, *o*-methyl, *o*-methoxy, *o*-piperidinyl, dramatically reduced or completely eliminated GKA potency (data not shown).

Investigation of the R_3 modifications of **1** resulted in improvements in potency, identified areas to introduce functionality, and provided clues regarding the active conformation required for GK activation. A significant increase in potency was observed upon introducing an *N*-methyl group at the terminal amide of **1**. Thus, analogue **5f** was about 5-fold more active than **1** (6 μM vs 29 μM). Combining one of the optimized groups at R_2, cyclopentyl, with an *N*-ethyl group at R_3 gave **5j** ($SC_{1.5}$ = 0.53 μM), one of the first GK activators with submicromolar potency. Further examination of the SAR of the terminal amide by introduction of larger *N*-alkyl groups, such as *n*-propyl, allyl, isopropyl, and *n*-butyl, led to a gradual decrease to complete loss of GKA potency (e.g. **5k**, **5l**, **5m**, and **5n**), reflecting the size limitations at R_3. For example, the acetate analogues **5o** and **5q** were about 6- to 8- fold more potent than the corresponding propionates **5r** and **5t**. The carboxylic acid analogues **5p** and **5s** were not active, while introduction of the hydroxyethyl group, **5u**, was well tolerated.

The optically pure *R*- and *S*-stereoisomers, **9a** and **9b** of racemic **5h**, were prepared as described in Scheme 2. The

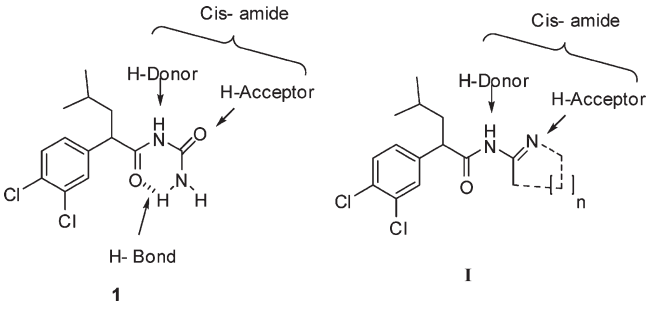

Figure 2. Intramolecular H-bond and *cis*-amide characteristics of **1** and the resulting 2-amino heteroaromatics hypothesis.

Table 2. Structure−Activity Relationships of 2-Aminothiazoleamides

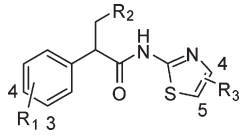

compd	R_1	R_2	R_3	$SC_{1.5}$ (μM)[a]
8a	3,4-diCl	cyclopentyl	H	0.94 ± 0.16 (2)
8b	3,4-diCl	phenyl	H	na
8c	3,4-diCl	cyclopentyl	4-methyl	1.2
8d	3,4-diCl	cyclopentyl	5-methyl	0.64
8e	3,4-diCl	cyclopentyl	4,5-dimethyl	1.6
8f	3,4-diCl	cyclopentyl	4-$COOC_2H_5$	2.7
8g	3,4-diCl	cyclopentyl	4-$COOCH_3$	0.5
8h	3,4-diCl	cyclopentyl	4-CH_2OH	0.99
8i	3,4-diCl	cyclopentyl	4-COOH	29
8j	3,4-diCl	cyclopentyl	5-$COOC_2H_5$	8
8k	3,4-diCl	cyclopentyl	5-COOH	26
8l	3,4-diCl	cyclopentyl	5-$COOCH_3$	0.92
8m	3,4-diCl	cyclopentyl	5-CH_2OH	0.75
8n	3,4-diCl	cyclopentyl	4-$CH_2COOC_2H_5$	0.61
8o	3,4-diCl	cyclopentyl	4-CH_2COOH	8
8p	3,4-diCl	cyclopentyl	4-CH_2COOCH_3	0.82
8q	3,4-diCl	cyclopentyl	4-CH_2CH_2OH	0.84
8r	4-Cl	cyclopentyl	H	3.1
8s	3-Cl	cyclopentyl	H	1.7
8t	4-NO_2	cyclopentyl	H	0.84
8u	4-SCH_3	cyclopentyl	H	2.2
8v	4-$S(O)CH_3$	cyclopentyl	H	2.2 ± 0.44 (2)
8w	4-SO_2CH_3	cyclopentyl	H	0.35 ± 0.022 (5)
8x	4-SCF_3	cyclopentyl	H	1.8
8y	4-SO_2CF_3	cyclopentyl	H	0.19 ± 0.057 (3)
8z	3-SO_2CF_3	cyclopentyl	H	1.4
21a[b]	4-SO_2CH_3	cyclopentyl	H	0.24 ± 0.019 (25)
21b[c]	4-SO_2CH_3	cyclopentyl	H	na

[a] Data reported as mean ± SEM (*n*). The average CV of the assay was 15%, based on an analysis of 452 compounds ($SC_{1.5}$ < 2 μM) assayed in duplicate. na: not active up to 30 μM. [b] *R*-isomer. [c] *S*-isomer.

absolute stereochemistry of **9a** was determined to be *R* on the basis of a single crystal X-ray structure (Figure 1 of Supporting Information). The *R*-isomer **9a** has an $SC_{1.5}$ of 0.41 μM, while the corresponding *S* isomer **9b** has no effect on GK activity at concentrations up to 10 μM. The crystal structure of **9a** further revealed that the *N*-acylurea moiety exists in a six-membered cyclic conformation characterized by an intramolecular H-bond, between the carbonyl of the acyl oxygen atom and the terminal NH of the urea, resulting in a cisoid conformation of the amide bond.

A variety of compounds were prepared to explore the significance of the *N*-acylurea conformation. In relation to

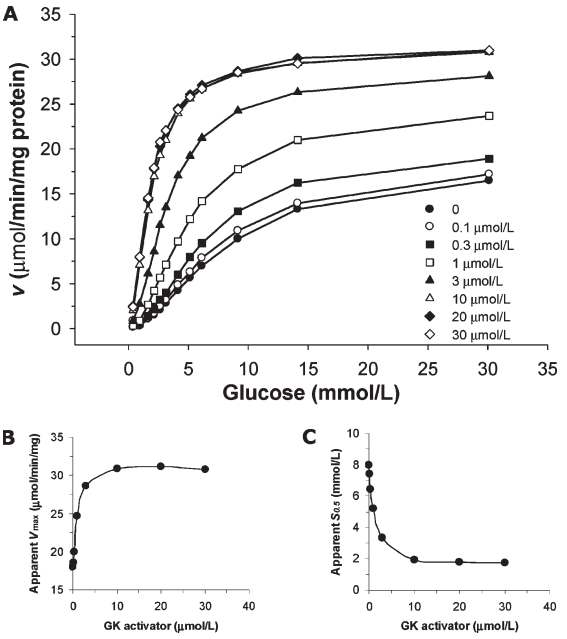

Figure 3. Effects of **9a** on GK kinetics: (A) rate versus glucose plot in the absence and presence of **9a**; (B) apparent V_{max} versus [**9a**]; (C) apparent $S_{0.5}$ versus [**9a**] plots.

5h, the cyclic urea **16**, the *N*-methylacylurea **18**, and the terminal *N*,*N*′-dimethyl analogue **19**, all of which lack the ability to make the intramolecular H-bond, failed to activate GK. The guanidine analogue **17**, which potentially could have an intramolecular H-bond but lacks the urea carbonyl that may accept a hydrogen bond from glucokinase, also failed to activate GK. The thiourea analogue **20** ($SC_{1.5}$ = 3.8 μM) lost about 4-fold in potency relative to the urea **5h** possibly as a reflection of the lower capacity of the sulfur atom to accept a hydrogen bond. The C_α-methylated analogue **15** (1-[3-cyclopentyl-2-(3,4-dichlorophenyl)-2-methylpropionyl]-3-methylurea) was found to be inactive, which suggested a potential steric effect between the C_α-methyl and the *N*-acylurea moiety, preventing it from making an optimal interaction with GK. Collectively, these observations suggested that the cyclic, intramolecularly hydrogen-bonded conformation adopted by the *N*-acylureas was necessary to support donor−acceptor hydrogen bonding with GK.

Later, the molecular modeling experiments with the *N*-acylurea GK activators using the X-ray co-crystal structures of other GK activator-GK identified key H-bond interactions with the backbone NH and carbonyl of Arg^{63} residue in GK.[11] These observations led to a hypothesis that amides derived from heterocyclic amines of formula **I** could mimic the H-bond donor−acceptor interactions of the *N*-acylurea's *cis*-amide bond (as shown in Figure 2). Several phenylacetamides of various 2-amino-nitrogen heteroaromatic systems were evaluated as GKAs and found to be active. In the following section, the SAR related to 2-aminothiazolephenylacetamide GKAs is described in detail and the data are summarized in Table 2.

In general, the SAR at R_1 and R_2 parallels the *N*-acylureas. Thus, the cyclopentyl analogue **8a** was very potent while the corresponding aryl derivative **8b** was significantly less active. To explore the thiazole SAR, **8a** was used as a positive comparator. Several 4- and 5-substituted thiazole analogue pairs were prepared to explore the optimal position to introduce functionality. As the data in Table 2 illustrates,

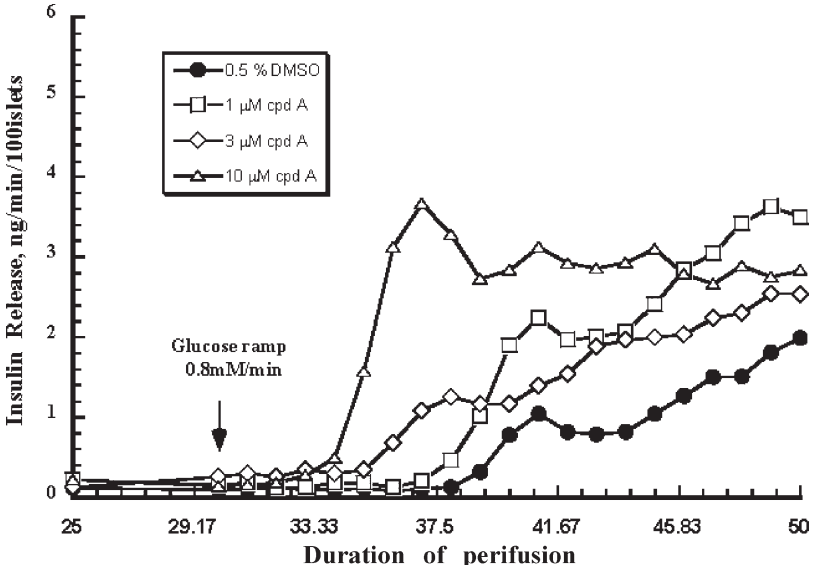

Figure 4. Compound **9a** (cpd A) lowers the threshold for glucose stimulated insulin release: effects of **9a** (cpd A) in isolated mouse islets, cultured for 4−5 days in 10 mM glucose. Following a preperifusion phase with a balanced salt solution in the absence of glucose, a glucose ramp was applied from 0 to 20 mM (0.8 mM/min) in the presence of the test agent. There were two to four replicates for each condition. Adapted from ref 14.

Table 3. *In Vitro* GK Enzyme Kinetics Data for Compounds **9a** and **21a**

	9a	**21a**
Parameter: V_{max} (μmol/min/mg protein)		
control	18.0	19.1
1 μM activator (fold change vs control)	24.7 (1.4)	23.7 (1.2)
20 μM activator (fold change vs control)	31.2 (1.7)	26.1 (1.4)
Parameter: $S_{0.5}$ (mmol/L)		
control	8.0	8.7
1 μM activator (fold change vs control)	5.2 (0.66)	3.3 (0.38)
20 μM activator (fold change vs control)	1.8 (0.22)	0.84 (0.10)

Table 4. Rat Pharmacokinetics Data for Compounds **9a** and **21a**

compd	dose (mg/kg)	route	Cl ((mL/min)/kg)	V_{ss} (L/kg)	AUC_{0-inf} (ng·h/mL)	C_{max} (μg/mL)	T_{max} (h)	F_{po} (%)
9a	5	iv[a]	43.48	4.21	1877			
	10	po[b]			455	133	1.4	12
	30	po[b]			1464	471	3.3	13
21a	5	iv[a]	30	2.16	2774			
	10	po[b]			5150	1140	3.3	92.8
	30	po[b]			51748	4302	4.7	311

[a] Formulation: 10% PEG-400. [b] Formulation: gelucire.

introduction of a methyl group at position 5 (**8d**) or at position 4 (**8c**) and 4,5-dimethyl (**8e**) thiazole analogues were not significantly different compared to **8a**. Although the presence of an ethoxycarbonyl at the 4- or 5-position (**8f** and **8j**) resulted in significant reduction in potency, the corresponding methoxycarbonyl derivatives **8g** and **8l** were equipotent to **8a**. The 4-acetic acid esters **8n** and **8p** and the hydroxyethyl analogue **8q** were all equipotent versus **8a**. All carboxylic acid containing analogues (**8i** and **8k**) were inactive. Thus, these observations identified areas to introduce polarity into the GK activator molecule to improve their solubility (solubility in water: **8a**, 5 μg/mL; **8g**, 24 μg/mL) and other "drug-like" properties.

The potency of R_1 analogues 4-nitro **8t**, 4-methylsulfonyl **8w**, and 4-trifluoromethylsulfonyl **8y** and the gradual potency improvement observed when comparing the thioether **8u**, methyl sulfoxide **8v**, and methylsulfone **8w** ($SC_{1.5}$ of 2.2−0.35 μM) analogues clearly suggested preference for electron withdrawing group(s) at R_1. Similar to *N*-acylureas, the *R* stereoisomer **21a** activated GK with a $SC_{1.5}$ of 0.24 μM while the corresponding *S* isomer **21b** did not activate GK up to 10 μM.

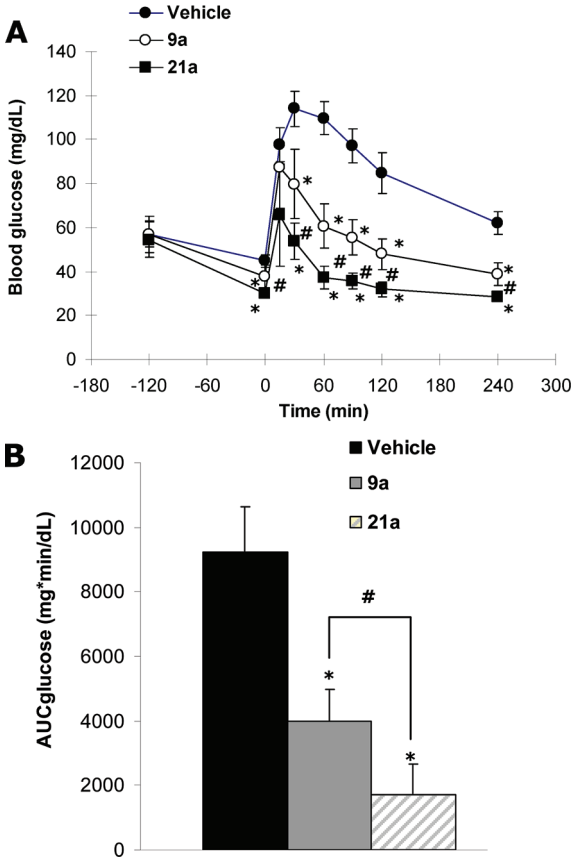

Figure 5. Acute effects of orally administered **9a** (50 mg/kg) and **21a** (50 mg/kg) on an oral glucose tolerance test in male C57BL/6J mice. All results are reported as the mean ± STD (n = 6/time point). A Student's t test was used to test for statistical significance: (*) $P < 0.05$ compared to vehicle; (#) $P < 0.05$ between **9a** and **21a**.

On the basis of SAR studies, the structural elements required in a phenylacetamide based GK activator can be summarized as follows: (i) an electron withdrawing substituent is necessary at R_1; (ii) a five- or six-membered alicyclic ring is optimal at R_2; (iii) a hydrogen bond donor−acceptor pair as part of an *N*-acylurea or an amide of 2-amino heterocycle with a H-bond acceptor capability (Figure 2) is required at R_3; (iv) the *R*-stereochemistry at the chiral center is needed.

***In Vitro and in Vivo* Activity Profile of Compounds 9a and 21a.** Extensive evaluation of several analogues for their *in vitro* potency and *in vitro* safety assessment assays led to the selection of **9a** and **21a** as advanced lead molecules. Consistent with the pancreatic β-cell hypothesis, these glucokinase activators have been shown to augment insulin release in studies conducted in freshly isolated rodent pancreatic islets and in pancreatic cell lines.[5,11] In general, glucokinase activators shift the glucose stimulated insulin release (GSIR) threshold to the left in a concentration-dependent and glucose-dependent manner. Glucokinase activator concentrations associated with cellular activity ranged from submicromolar to low micromolar range and can vary depending on the assay conditions and glucose levels (vide supra). Compound **9a** dose-dependently increased the enzymatic activity of GK across a wide range of glucose concentrations (Figure 3), whereas the corresponding *S*-enantiomer was inactive (not shown). Activation of GK was driven by dual effects of increasing the enzyme's V_{max} (Figure 3B) and lowering its $S_{0.5}$ (concentration of glucose at half-maximal velocity) for glucose (Figure 3C). The magnitude of these effects at 1 and 20 μM activator concentration was determined by fitting the data to the Hill equation (Table 3). Compound **9a** exerted a relatively larger increase in V_{max} (1.7-fold change for **9a** versus 1.4-fold change for **21a** at 20 μM), whereas **21a** showed a greater effect on reducing the enzyme's $S_{0.5}$ for glucose (1.8 mmol/L for **9a** versus 0.84 mmol/L for **21a** at 20 μM activator concentration).

Consistent with the role of pancreatic β-cell GK, treatment of rodent islets with **9a**[14] (Figure 4) or **21a**[5] shifted the glucose-stimulated insulin release curve to the left as demonstrated in perifusion studies using isolated pancreatic islets. To better discriminate between the two GK activators, head-to-head *in vivo* efficacy studies were performed. Oral administration of **9a** and **21a** (50 mg/kg) to male C57Bl/6J mice caused a statistically significant reduction in fasting glucose levels and improvement in glucose tolerance relative to the vehicle treated animals (Figure 5A). Compound **21a** showed a statistically significant superior effect during the oral glucose tolerance test (OGTT) relative to **9a** (Figure 5B). Comparison of rat PK parameters indicated that **21a** displayed lower clearance and higher oral bioavailability compared to **9a** (Table 4). Oral bioavailability of the 30 mg/kg **21a** dose exceeded 100% probably as a result of precipitation at the injection site or insufficient sampling following iv administration and the consequent failure to fully capture the distribution phase. Other possibilities (saturable hepatic first-pass clearance or gut wall metabolism) cannot be excluded. The PK properties of orally administered **21a** were similar between the gelucire solution and klucel suspension. Oral bioavailability in dog and monkey was 109% and 67%, respectively, using Klucel (hydroxypropylcellulose)[12] suspension.

On the basis of the outcome of a 5-day repeat-dose toxicity studies conducted in rats, **21a** was chosen over **9a** for further development and advancement into single ascending dose trials in healthy volunteers. Following a single oral dose, **21a** reduced fasting and postprandial glucose levels following an OGTT, was well tolerated, and displayed no adverse effects related to drug administration other than hypoglycemia at the maximum dose (400 mg), which defined the maximum tolerated dose.[13]

Conclusion

In summary, we have discovered two potent allosteric GK activator molecules, **9a** and **21a**, based on the optimization of a unique *N*-acylurea hit molecule **1**. The results of the SAR work established a useful pharmacophore model that we exploited in the design of several potent glucokinase activators including **21a**, the one that we used to demonstrate the clinical relevance of targeting GK for the treatment of T2D.

Acknowledgment. The authors thank Dr. Jefferson Tilley for helpful discussions. The authors are grateful to Dr. Anthony Greway for DMPK support, Linda Marcus for the GK activity assays, and Dr. Amy Sarjeant for the compound **9a** X-ray structure determination. The authors are also grateful to all members of the Department of Physical Chemistry, Hoffman-La Roche, for the characterization of the compounds.

Supporting Information Available: Experimental procedures and analytical data for all intermediate and final compounds. This material is available free of charge via the Internet at http://pubs.acs.org.

References

(1) De Fronzo, R. A. From the triumvirate to the ominous octet: a new paradigm for the treatment of type 2 diabetes mellitus diabetes. *Diabetes* **2009**, *58*, 773–795.
(2) Matschinsky, F. M. Assessing the potential of glucokinase activators in diabetes therapy. *Nat. Rev. Drug Discovery* **2009**, *8*, 399–416.
(3) Grimsby, J.; Berthel, S. J.; Sarabu, R. Glucokinase activators for the potential treatment of type 2 diabetes. *Curr. Top. Med. Chem.* **2008**, *8*, 1524–1532.
(4) Coghlan, M.; Leighton, B. Glucokinase activators in diabetes management. *Expert Opin. Invest. Drugs* **2008**, *17*, 145–167.
(5) Grimsby, J.; Sarabu, R.; Corbett, W. L.; Haynes, N. E.; Bizzaro, F. T.; Coffey, J. W.; Guertin, K. R.; Hilliard, D. H.; Kester, R. F. K.; Mahaney, P. E.; Marcus, L.; Qi, L.; Spence, C. L.; Tengi, J.; Magnuson, M. A.; Chu, C. A.; Dvorozniak, M. T.; Matschinsky, F. M.; Grippo, J. F. Allosteric activators of glucokinase: potential role in diabetes therapy. *Science* **2003**, *301*, 370–373.
(6) (a) Bertram, L. S.; Black, D.; Biner, P. H.; Chatfield, R.; Cooke, A.; Fyfe, M. C. T.; Murray, P. J.; Naud, F.; Nawano, M.; Procter, M. J.; Rakipovski, G.; Rasamison, C. M.; Reynet, C.; Schofield, K. L.; Shah, V. K.; Spindler, F.; Taylor, A.; Turton, R.; Williams, G. M.; Wong-Kai-In, P.; Yasuda, K. SAR, pharmacokinetics, safety, and efficacy of glucokinase activating 2-(4-sulfonylphenyl)-*N*-thiazol-2-yl-acetamides: discovery of PSN-GK1. *J. Med. Chem.* **2008**, *51*, 4340–4345. (b) Efanov, A. M.; Barrett, D. G.; Brenner, M. B.; Briggs, S. L.; Delaunois, A.; Durbin, J. D.; Giese, U.; Guo, H.; Radloff, M.; Gil, G. S.; Sewing, S.; Wang, Y.; Weichert, A.; Zaliani, A.; Gromada, J. A novel glucokinase activator modulates pancreatic islet and hepatocyte function. *Endocrinology* **2005**, *146*, 3696–3701. (c) Castelhano, A. L.; Dong, H.; Fyfe, M. C. T.; Gardner, L. S.; Kamikozawa, Y.; Kurabayashi, S.; Nawano, M.; Ohashi, R.; Procter, M. J.; Qiu, L.; Rasamison, C. M.; Schofield, K. L.; Shah, V. K.; Ueta, K.; Williams, G. M.; Witter, D.; Yasuda, K. Glucokinase-activating ureas. *Bioorg. Med. Chem. Lett.* **2005**, *15*, 1501–1504.
(7) Sarabu, R.; Berthel, S. J.; Kester, R. F.; Tilley, J. W. Glucokinase activators as new type 2 diabetes therapeutic agents. *Expert Opin. Ther. Pat.* **2008**, *18*, 759–768.
(8) Karmouta, M. G.; Miocque, M.; Derdour, A.; Gayral, P.; Lafont, O. Synthse de cyanacetylurees en vue d'essais vis-a-vis d'hymenolepisnana. *Eur. J. Med. Chem.* **1989**, *24*, 547–549.

(9) Wiley, P. F. The reaction of amides with isocyanates. *J. Am. Chem. Soc*. **1949**, *71*, 1310–1311.
(10) Froyen, P. The conversion of carboxylic acids into amides via NCS/triphenylphosphine. *Synth. Commun*. **1995**, *25*, 959–968.
(11) Dunten, P.; Swain, A.; Kammlott, U.; Crowther, R.; Lukacs, C. M.; Levin, W.; Reik, L.; Grimsby, J.; Corbett, W. L.; Magnuson, M. A.; Matschinsky, F. M. Crystal Structure of Human Liver Glucokinase Bound to Small Molecule Allosteric Activator. In *Glucokinase and Glycimic Disease. From Basics to Therapeutics*; Matschinsky, F. M., Magnuson, M. A., Eds.; Karger AG: Basel, Switzerland, 2004; pp 145−154.
(12) Guo, J.-H.; Skinner, G. W.; Harcum, W. W.; Barnum, P. E. Pharmaceutical applications of naturally occuring water-soluble polymers. *Pharm. Sci. Technol. Today* **1998**, *1*, 254–250.
(13) Grimsby, J.; Zhi, J.; Mulligan, M. E.; Arbet-Engels, C.; Taub, R.; Balena, R. Antidiabetic Effects of Glucokinase Activators: From Benchside to Bedside. Presented at the Keystone Symposia: Diabetes Mellitus, Insulin Action and Resistance, Breckenridge, CO, January 22−27, **2008**; Poster No. 151.
(14) Grimsby, J.; Mastschinsky, F. M.; Grippo, J. F. Discovery and Actions of Glucokinase Activators. In *Glucokinase and Glycemic Disease: From Basics to Novel Therapeutics*; Matschinsky, F. M., Magnuson, M. A., Eds.; Karger AG: Basel, Switzerland, 2004; pp 360−378.